BACHELOR

The influence of coater velocity on layer deposition in the 3D-printing process

Groot, Niek

Award date:
2019

TU/e

Bachelor end project

3CEX0

The influence of coater velocity on layer deposition in the 3D-printing process

Author:
Niek Groot (1018809)

Supervisors:
Andrei Kozhevnikov
Herman Clercx

R-1978-B

July 5, 2019

Abstract

Additive manufacturing, also known as 3D-printing, is an upcoming technology. This thesis will focus on a specific form of additive manufacturing, namely vat photopolymerization. In this process a thin layer of resin is deposited and partly solidified. After a layer is deposited, a new layer is added. This process is repeated until the product is ready. This specific type of additive manufacturing has as a main advantage that it is possible to 3D-print ceramic objects. However, there are still some challenges to overcome for this method to work perfectly. One of these challenges is that small deformations can be developed during the layer deposition process. When these deformations are stacked on top of each other they can cause imperfections in the object that is being 3D-printed.

In this thesis the Lepus Next Gen, a vat photopolymerization machine from TNO, is used to address the search for parameters that have a effect on the flow and thereby on the height profile of the deposited layer. The main parameters which are investigated are the coater height above the bottom plate and the coater velocity. To investigate these parameters firstly a formula is derived to predict the height profile of a deposited layer. This is done by using the Navier Stokes equation for a simplified geometry. the derived formula is tested experimentally. Furthermore, the gathered results are compared with simulations based on Comsol.

To conclude this thesis it is found that the experimentally found height profiles agree quite well with the analytical predictions for most of the measured coater velocities and coater heights above the bottom plate. Furthermore it is found, that those height profiles are consistent with the predicted height profiles by the Comsol based model to a large extent.

Contents

1 Introduction

To create an object a lot of methods can be used, such as welding, casting etc. Most of these techniques have already existed for a very long time. However, a new method is emerging very rapidly, additive manufacturing, also known as 3D-printing. It is especially useful when trying to make very specific one-of-a-kind objects with unique geometry. 3D-printing works on a very simple principle. One will have some kind of raw substance, mainly polymers, which can be easily moved to the desired position where parts of it can be solidified in some way. This thesis' main focus is vat photopolymerization. This method is based on creating a very thin layer of resin, which is essentially a liquid polymer which can be solidified with a laser, so that it can be subsequently locally solidified. After the solidification, a new layer is added which again is solidified. This process is repeated until the desired end product is printed. The specific form of vat photopolymerization, which will be focused on in this thesis, is the printing process of large area ceramics. This printing process uses the same techniques as vat photopolymerization. However, in this specific process ceramic particles are added to the raw substance, hereby creating a resin consisting of polymers and ceramic particles. When using this process, one will end up with an object made out of polymers and ceramic particles. Finishing the product and truly making a large area ceramic will be done by sintering the 3D-printed object. Sintering is the process of placing the 3D-printed object in an oven which will melt away the polymers and strengthen the bonds between the small ceramic particles. This finally makes the object fully ceramic.

However, as easy as this process sounds, there are still some issues with this process that need to be addressed. Most of the problems concern the layer-by-layer approach of the building process. The first problem of the layer-by-layer process is that layers should stick to each other, which is not always the case. The second problem to be dealt with is that it is very hard to create a perfectly flat layer, especially when some parts of previously deposited layers are not solidified and remain liquid. This is already a problem of its own, but it becomes an even bigger problem when more layers are added, causing errors to be stacked on top of each other. This can often cause structural imperfections and errors in the shape of the product.

To solve this problem, work is being done to develop a control system to

reduce the effect of errors stacking on top each other. This is done in such a way that structural integrity and shape of the product are preserved. The main goal of this thesis is to determine some parameters which could be adjusted to control the resin flow and resin layer thickness, during the coating process.

2 Research tasks

For this Bachelor end project two main tasks will be treated. Firstly, the influence of the coater velocity and coater height above the bottom plate on the height profile of the deposited layer will be tested experimentally. The height profile is a measurement of the height along the moving axis of the coater. A typical height profile will look like a graph where one axis will show the height of the resin and the second axis will show the coordinate along the moving axis of the coater. Secondly, in a computational fluid dynamics (CFD) model proposed by Kozhevnikov and coworkers an assumption is made that the problem can be modeled as a two-dimensional one [7]. This assumption will be tested.

To correctly achieve these goals a plan has to be made on how to carry out measurements which will provide a correct and consistent answer on the questions stated in the previous paragraph. To determine the influence of coater velocity on the height profile of the resin, several measurements will be performed. Measurements will be done along the moving axis of the coater, while keeping the height of the coater constant, with different velocities. For these different velocities the height profile of the resin will be measured with a co-moving sensor at a fixed distance behind the blade. Similarly the measurements with different coater velocities will be performed on different coater heights, in order to precisely determine the influence of the coater velocity and coater height on the resin height profile.

To evaluate the results gathered by the previously mentioned measurements, a comparison will be made with the CFD model. This comparison will consider mainly the height profile measured during the experiment and the height profile gathered by using the model, while using the same measurement configuration. This can give insights into the flow physics of layer deposition.

The CFD model assumes that the process of layer deposition is a symmetric problem. This assumption allows the model to be reduces to two dimensions. In order to check if the 2D-model assumption is correct, different measurements of the height profile along the moving axis of the coater will be performed. However, this time the measurements will be done at different spanwise positions. The measurements of the height profile will be performed along the symmetry axis 10 mm right of the symmetry axis and

10 mm to the left of the symmetry axis. After several measurements of the height profile have been performed, all results from different spanwise positions will be compared to each other. If all measurements show the same height profile, the assumption of a 2D-model will be appropriate. However, these measurements of the height profiles should be performed under equal conditions to make the results credible. To achieve this goal, a dry measurement will be performed first. A dry measurement is a measurement without any resin. This will make sure that any imperfections in the bottom plate will be spotted and can be taken into account.

Another very important aspect to keep in mind is the method of deposition of the resin in front of the coater before each measurement. In the model proposed in [7], the coater is partly submerged in the perfectly flat liquid layer. This makes sure that there is an abundance of resin available. Furthermore, this causes the resin to be equally spread when starting the coating process. Because of this process the amount of resin and the spread of the resin will be consistent during every measurement.

Performing measurements as described above will make sure they will be performed in equal manner. This ensures gaining the results necessary to draw useful conclusions regarding the research tasks stated earlier.

3 Background information

3.1 Large area ceramics by additive manufacturing

In this thesis the main focus is on the prototype printing system, called the Lepus Next Gen. This system is being developed by AMSYSTEMS[1]. The goal, which AMSYSTEMS hopes to achieve with the Lepus Next Gen, is to make a 3D-printer which can print large area ceramics. The process of printing large area ceramics works by depositing one layer of resin which consists of polymers and ceramic particles. The layer deposition works by adding a certain amount of resin in front of a coater, which will then spread the layer as evenly as possible. If the resin is not spread out evenly, errors can occur, which can make the entire product useless. After a layer has been deposited the desired parts of the layers can be solidified using a laser. When the desired part of the layer has been solidified, another layer is added. This will again be partly solidified. This process will be repeated until the desired object is created.The end product of this process is called the green part. However, the green part is not yet the end product, because the green part still contains polymers and is not fully ceramic. To make the object fully ceramic it has to be sintered. Sintering is the process of placing the 3D-printed object in an oven which will melt away the polymers and strengthen the bonds between the small ceramic particles. This makes the object fully ceramic.

3.2 Layer deposition

As explained before, the way layers are added is by using a coater. The coater can be considered as a bar spreading resin out in thin layers on the desired surface. This is not as easy as it sounds, because layers do not always stick to one another and an even bigger problem is the fact that most layers do not have a perfectly flat surface and desired thickness. To fully understand this problem, a better look will be taken at the physics of layer deposition. A schematic view of this process is shown in figure 1.

[1] sub-organisation of TNO

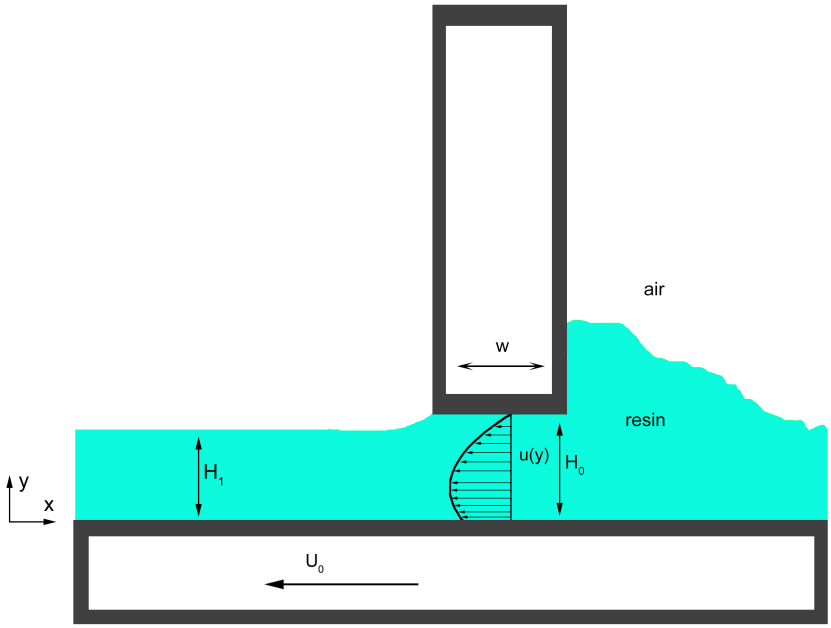

Figure 1: A schematic view of the process of layer deposition in which the velocity profile can be seen in between the coater blade and the bottom plate

When the coater is moving to spread the resin it will induce a flow within the resin. In fact, the flow is a combination of two basic flows. One of them is pressure driven. The pressure is created by a bulge of resin before the coater blade. The other component is shear driven. The shear is created by the moving coater blade. Therefore, the total velocity profile will be a mix of a Poiseuille and a Couette velocity profile. To derive the velocity profiles inside the resin beneath the coater, the Navier-Stokes equation will be used, for a Newtonian and incompressible fluid, which is given in equation (1) [8]. Here, ρ is the density, $\vec{u}$ the flow velocity, P the pressure, μ the dynamic viscosity and $g = -g\hat{y}$ the gravity

$$\rho \frac{D\vec{u}}{Dt} = -\nabla p + \mu \nabla^2 \vec{u} + \rho \vec{g}. \tag{1}$$

This equation can be simplified if some assumptions are made. It will be assumed that flow is fully developed beneath the moving blade. The assumption of a fully developed flow can only be made for the case $W \gg H_0$, which is not always true during the coating process. Therefore, one should

consider if the formula which is derived is applicable.In our case the Navier-Stokes equation can be reduced to the following simplified form.

$$\frac{\partial P}{\partial x} = \mu \frac{\partial^2 u}{\partial y^2}. \tag{2}$$

If the no-slip boundary condition is applied at the walls, and mass conservation is taken into account, one can derive a velocity profile for the flow beneath the coater. The velocity profile is given in equation (3), where $u(y)$ is the velocity profile, U_0 is the velocity of the coater and H_0 the height of the coater above the bottom plate.

$$\frac{u(y)}{U_0} = \frac{1}{2\mu U_0} \frac{\partial P}{\partial x} y(y - H_0) + (\frac{y}{H_0} - 1). \tag{3}$$

For this derivation a comoving frame of reference is used. The main difference for the derivation is the fact that in the comoving frame the bottom plate is moving to the left with velocity U_0 instead of the coater which is moving to the right in practise. All other variables have their usual meaning. The velocity profile is sketched in figure 1. To simplify the velocity profile (3), three dimensionless parameters will be introduced.

$$\Phi(y) = \frac{u(y)}{U_0} \tag{4}$$

$$\Pi = \frac{{H_0}^2}{2\mu U_0} \frac{\partial P}{\partial x} \tag{5}$$

$$\epsilon = \frac{y}{H_0} \tag{6}$$

This simplification can be done by substituting these three dimensionless parameters into equation (3). Furthermore, one of these three dimensionless parameters will prove to be very useful later on in this thesis [3]. When the dimensionless parameters are substituted into equation (3), equation (7) is obtained. This equation can be used to determine the height of the deposited layer of resin.

$$\Phi = \Pi(\epsilon^2 - \epsilon) + \epsilon - 1 \tag{7}$$

To determine the height of the layer of resin, mass conservation in the x-direction can be used. Mass conservation states that the mass fluxes at two different points in the flow should be equal. The total mass flow in the x-direction behind the coater is $Q_1 = -H_1 U_0$ and the mass flow beneath the coater is $Q_0 = \int_0^{H_0} u(y)dy$. When applying the law of mass conservation, a formula for H_1, the height of a layer, emerges. $H_1 = \frac{-\int_0^{H_0} u(y)dy}{U_0}$. However, this formula can be simplified substantially by again introducing the dimensionless parameters (4), (5) and (6). When solving the integral in the formula with substituted parameters, the following formula emerges,

$$\frac{H_1}{H_0} = \frac{\Pi}{6} + \frac{1}{2}. \tag{8}$$

3.3 Dimensionless parameters

As previously mentioned, dimensionless parameters can be useful when describing the layer deposition problem. The previously mentioned parameter Π gives the relation between pressure forces and viscous forces as described in equation (5). When the dimensionless parameter Π is known, a lot of information will be available about the layer deposition problem. For instance, it is very easy to predict the velocity profile and the thickness of the resin layer when the dimensionless parameter Π is determined. When the dimensionless parameter is small, say $\Pi \gg 3$, the Couette velocity profile will be dominant. This will cause a resin layer of about half the coater height. However, when the dimensionless parameter becomes much larger, the Poiseuille velocity profile will take over the dominant role. For this to happen, it should be that $\Pi \gg 3$. This also means that the resin layer thickness will increase. When taking a look at equation (8) one can see that a tipping point will be encountered when the dimensionless parameter reaches a value of $\Pi = 3$. The tipping point indicates the point where the dominant flow switches between a Couette and a Poiseuille flow. At this point both the Couette and Poisseuille flow will be noticeably present. When the dimensionless parameter reaches the value three the resin thickness will be exactly equal to the height of the coater. In figure 2 the effect of the dimensionless parameter on the velocity profile and the resin thickness can be seen. From the analysis of this problem it can be concluded that the dimensionless parameter Π, the ratio between pressure forces and viscous forces, can be used to determine the flow characteristics of this problem [3].

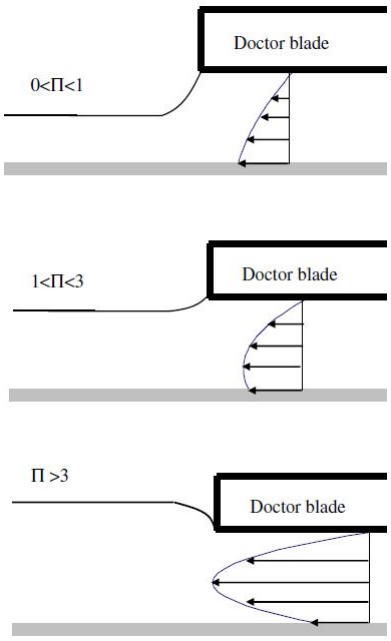

Figure 2: An overview of the velocity profile beneath the coater and resin thickness depending on Π with courtesy to [3].

3.4 Height sensors

For this thesis, measuring the height of the resin is very important. The data of measuring the height can give all information needed for the results if experiments are carried out successfully. However, a very important question which needs to be answered is which type of height senor will be most suitable for measuring the height of the resin layer. Of course, a ruler would not be precise enough, since the desired thickness will be around $100\mu m$, and this cannot be measured by a ruler. Furthermore, a contactless height sensor is necessary otherwise the layer can be influenced by the height sensor itself. For this thesis two main senors will be considered, the laser triangulation sensor and the confocal chromatic sensor. Both sensors will be explained more thoroughly in this chapter.

3.4.1 Laser triangulation sensor

The laser triangulation sensor works on a very simple principle, as the name already suggests; triangles. To measure the distance between the sensor and

a certain object, the sensor will target a laser beam on the object. This object will reflect the laser light and some of the reflected light will return to the sensor. The angle of the returning light will be measured at a point right next to the laser. From this angle the distance between the laser and the object can be determined. For most cases a resolution of 0.03 μm can be reached [1]. A schematic representation of a laser triangulation sensor can be seen in figure 3.

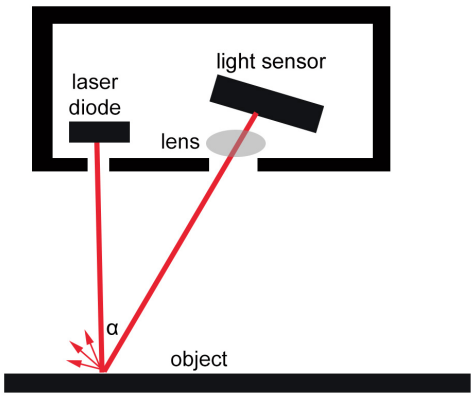

Figure 3: A schematic view of a laser triangulation sensor.

However, as nice as this idea might seem, in practice using a laser triangulation sensor is a little more complicated. One of the main downsides of the laser triangulation method is the fact that the accuracy of the measurement strongly depends on properties of the object's surface, such as reflectively, transparency and color. The accuracy of the sensor deteriorates when trying to measure a transparent liquid. The resolution can be increased by making the liquid opaque. Therefore the laser triangulation sensor will be deemed insufficient for the application considered in this thesis [6], [1].

3.4.2 Confocal chromatic sensor

The confocal chromatic sensor works on a somewhat more complicated principle. It works on aberrations in optics, specifically the chromatic aberration. For most optical setups this aberration is unwanted, but for this sensor the aberration is essential. This aberration says that the refractive index of a refracting object is dependent on the wavelength of the light passing through. This means that different wavelengths will have different focal points when

passing through the lens. The effect of the chromatic aberration on a poly-chromatic light source can be seen in the sketch displayed in figure 4.

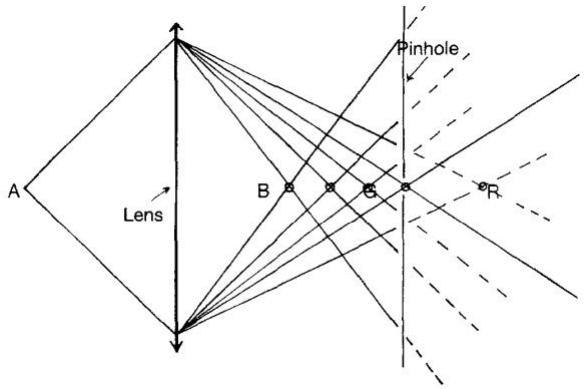

Figure 4: A schematic representation of chromatic aberration, where A is a polychromatic light source and B,G and R are the focal points of red, blue and green light. With courtesy to [2].

A formula for the depth of focal point $i$is given in equation (9) in which b and c are setup dependent constants, λ_0 the wavelength with its focal point closest to the lens and denotes a certain wavelength [2].

$$\Delta(i) = b(\lambda_i - \lambda_0)^c \tag{9}$$

As one can see in equation (9), the focal point will lie further away from the lens if the wavelength becomes larger. When projecting a poly-chromatic light source on an object using a lens, light will be reflected. However, since a lens in which the chromatic aberration is noticeable will be used, different wavelengths will be reflected differently. The wavelength which has its focal point exactly at the object's surface, will be reflected most strongly. When measuring the reflected light, it will be easy to identify which wavelength is most strongly reflected. By applying equation (9) to this wavelength, the distance from the sensor to the object can be determined.

The focal chromatic sensor has a resolution which is a little worse than the laser triangulation method. However, when measuring the height of an object it does depend less on what type of surface is being scanned. When trying to measure the distance to a fluid surface the confocal chromatic sensor will have a higher accuracy. The resolution of a confocal chromatic sensor is 3

nm. However, when scanning a transparent surface this will reduce to 3 μm [5]. Unfortunatly, the confocal chromatic sensor also has some disadvantages. The confocal chromatic sensor is more expensive and it is slower than the laser triangulation sensor [5], [1].

When comparing the laser triangulation sensor with the confocal chromatic sensor it becomes clear immediately that the confocal chromatic sensor is more precise. Unfortunately, the confocal chromatic sensor is a little slower and more costly than the laser triangulation sensor. Still, the confocal chromatic sensor will be used, since its precision is deemed necessary for this investigation.

3.5 CFD model

As previously mentioned, a comparison between the computational fluid dynamics (CFD) model and the experimentally found results will be made [7]. For clarity the CFD model will be explained briefly in this thesis. For this model a CFD package called Comsol is used. Comsol uses finite element discretization and is able to adapt the quality of the mesh depending on changing geometry and the necessity of a good resolution. This increases the accuracy and decreases the time necessary to run the model. In this model the phase field technique is used to model the interface of resin and air. The phase field method works by substituting the boundary conditions at the interface with partial differential equations for the evolution of an auxiliary field that takes the role of an order parameter. This technique makes sure the surface tension and the gravity are taken into account [9]. An interfacial layer is used to trace the resin-air interface. Furthermore, it is assumed that the flow of resin is Newtonian and incompressible, for the same reasons as in section 3.2.

4 Experimental setup

For this thesis an experimental setup was delivered by AMSYSTEMS, a sub-organization of TNO. The system is called the Lepus Next Gen. Most of the technical parts of the machine will not be discussed since they are irrelevant for the rest of this thesis. However, it will be explained how the setup works and in which way the experiments regarding the height profile will be performed. Furthermore, it will also be explained how the data which is measured using a confocal chromatic sensor is processed to get results.

4.1 Lepus Next Gen

As already mentioned, the Lepus Next Gen is used for this thesis. A schematic view of the most important components can be seen in figure 5. The confocal chromatic sensor will measure the distance between the sensor and the surface. The coater will be used to spread the resin in layers. The resin injector will make sure the right amount of resin will be available at any given time. This makes sure all experiments are carried out with equal conditions.

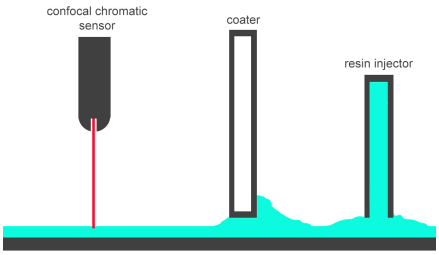

Figure 5: A schematic representation of the experimental setup which was used. The confocal chromatic sensor, coater and resin injector are all mounted to the same movable stage (not to scale).

A picture of the Lepus Next Gen is shown in figure 6. In the Lepus Next Gen the confocal chromatic sensor, the coater and the resin injector are all mounted to the same movable stage, which is mounted on the sides of the machine. This helps greatly during the measurements since the three components will always move together. The biggest advantage is that the confocal chromatic sensor can measure the height profile of the resin directly after it is deposited. Due to the decently high viscosity of the resin and the direct measurement after the layer deposition, settling effect will have limited

time to occur. This is one important aspect for the way the experiments discussed in this thesis are performed.

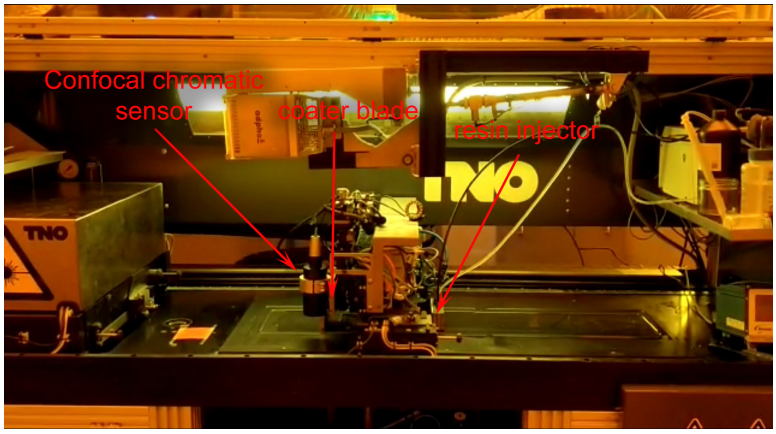

Figure 6: A picture of the Lepus Next Gen, where one can see the bottom plate and the movable stage containing the confocal chromatic sensor, coater and the resin injector. Courtesy AMSYSTEMS

However, as explained earlier in chapter 2, it has to be made sure that all experiments are performed with equal conditions. One of the conditions that should be paid attention to, is that there is the same amount of resin every time and that this resin has the same level before each measurement. To make sure this even spread of resin is achieved, first a layer of resin will be deposited by the resin injector. After the layer has been deposited, the coater blade will be submerged slightly in the resin and start spreading a new layer. This makes sure that the conditions of all the experiments are equal, because there will always be an abundance of resin, to be spread evenly. Another advantage is the fact that the model described in the CFD model in section 3.5 is based on a similar model. It also has a submerged blade as its initial position [7].

Another important aspect which should be taken into account is the fact that the bottom plate is not perfectly flat and that minor errors are present in the measurements performed by the confocal chromatic sensor. Error reduction can be achieved by measuring the height profile of the bottom plate before any resin is added. When processing the data, errors can be reduced by subtracting the measurement of the profile of the resin, from

the dry measurement. This will give the absolute value of the height profile removing most of the errors occurring due to bumps in the bottom plate or a deviation in the confocal chromatic sensor.

During this thesis two main problems are tackled. The first problem is to determine the influence of velocity on the height profile. To measure this height profile the height of the resin will be measured along a line parallel to the moving axis of the coater for different coater heights and coater velocities. The second problem is to check if the 2D assumption of the model is correct. In order to check this assumption it is made sure that the previously mentioned measurement, the measurement along the moving axis of the coater, is carried out three times, but at three different spanwise positions. The spanwise positions used in this thesis are 190 mm, 200 mm and 210 mm. Where 200mm is the symmetry axis and the 190mm and 210 positions are 10 mm to the left and right of the symmetry axis. The reason these numbers are so high is because of the way the axis system is defined in the Lepus Next Gen. The most important aspect to notice is that the measurements at different spanwise positions are 10 mm apart. A graphical representation of the measurements at different spanwise positions is shown in figure 7.

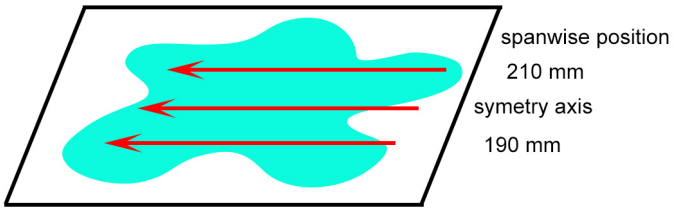

Figure 7: A grapical representation on the measurements at different spanwise positions (not to scale).

4.2 Flow and blade configuration for Comsol

Another experiment which is performed during this thesis is one using the Comsol model as described in [7]. This model is configured in such a way that all important parameters matched with those of the experiment which were performed using the Lepus Next Gen. The coater height is chosen to be 150 μm, the layer deposition takes place above a flat plate. Furthermore, the coater velocity is chosen to be 200 mm/s, the coater blade width is 10

mm and the viscosity 0.1 Pa·s. A figure of the model configuration is shown in figure 8.

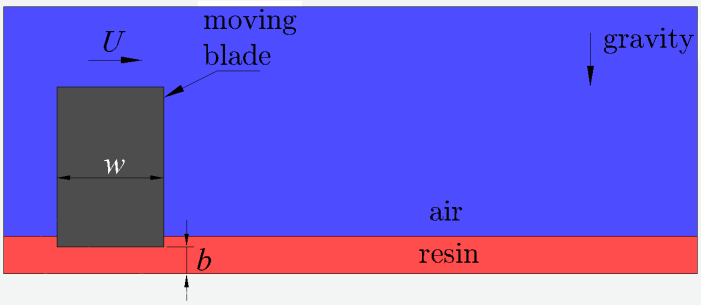

Figure 8: The Comsol model configured in a way to match the experiment as closely as possible, with U the coater velocity, W the coater width and b the coater height. Courtesy to Kozhevnikov (not to scale).

5 Results

In this chapter, the results of the performed experiments are displayed. First, the results of the Comsol model will be discussed. In section 5.2, the results of the various measurements which use the Lepus Next Gen will be shown. First a couple of height profile graphs will be shown and after this a table so relations can be seen better.

5.1 Results of the model

The model resulted in a resin layer of exactly half the coater height above the bottom plate. This result is expected, because this is exactly as formula (8) predicts. Since the coater velocity was relatively high and the coater height was relatively low the effects of change in viscosity and change of coater velocity were almost not noticeable when looking at the height profile.

5.2 Results of the experiment

For this thesis, several measurements have been performed as described in chapter 2. For each coater height there have been conducted five measurements with different coater velocity. This chapter will only include the graphs of measurements which have been performed at a coater height of 200 μm and tables of measurements which have been performed at a height of 200 μm. However, the complete list of results of all measurements which are performed can be found in Appendix B. The results for the measurement with a coater height of 200 μm are shown in figure 9. The panels show the absolute height profile of resin during each measurement.

To get a better insight into the height profiles the mean of the height profile and its standard deviation are shown in tables 4, 5 and 6 for different spanwise positions. These three tables only show the mean and standard deviation for the measurement of a coater height of 200 μm. The tables are perfect for noticing small differences between the measurements.

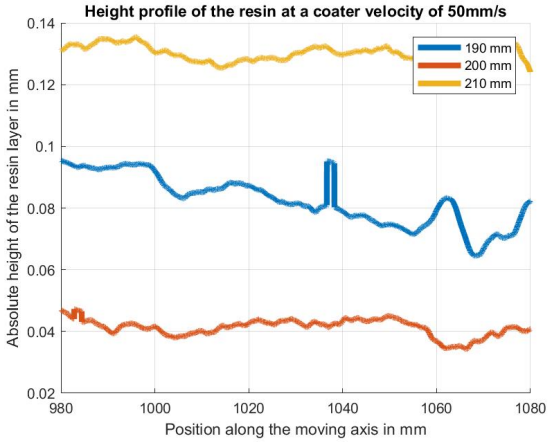

(a)

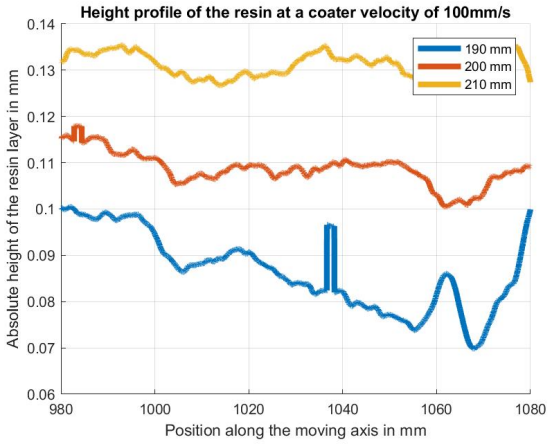

(b)

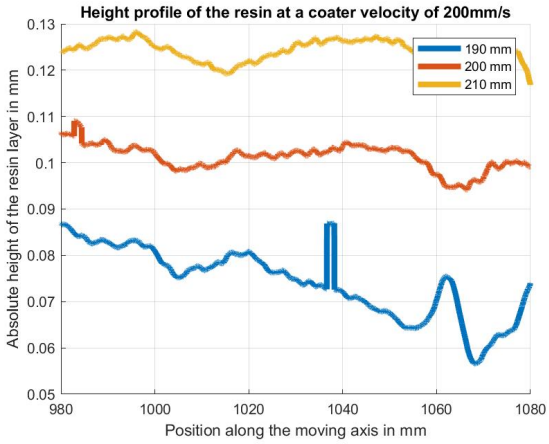

(c)

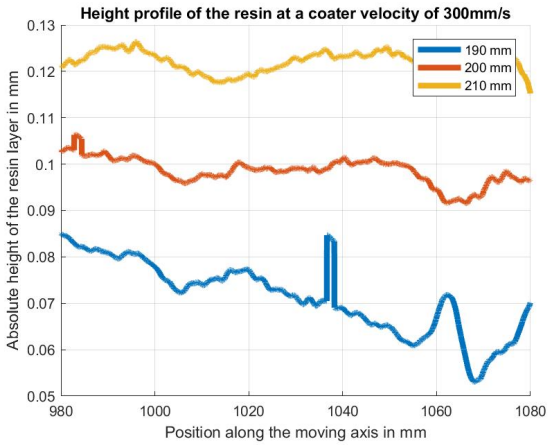

(d)

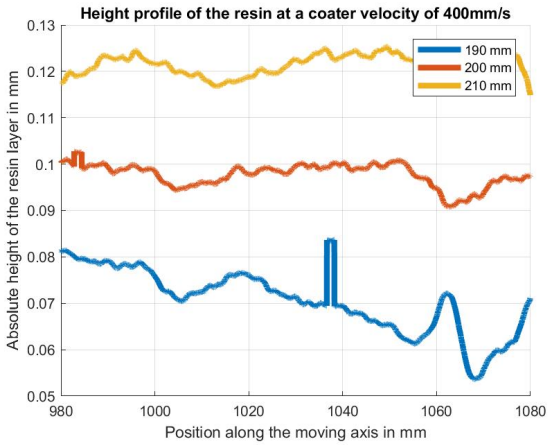

(e)

Figure 9: The absolute height profile of the resin with a coater height of 200 μm above the bottom plate, spanwise positions of 190 mm, 200 mm and 210mm and for five different velocities 50 mm/s, 100 mm/s, 200 mm/s, 300 mm/s and 400 mm/s. The spike in every 190 mm measurement is caused by a bump which was measured in the bottom plate.

Coater velocity	Mean of the height profile in μm	Standard deviation in μm
50 mm/s	82,4	8,2
100 mm/s	86,4	8,3
200 mm/s	74,1	7,5
300 mm/s	71,2	7,8
400 mm/s	70,5	6,9

Table 1: In this table the mean height profile and standard deviation for spanwise position 190 are shown.

Coater velocity	Mean of the height profile in μm	Standard deviation in μm
50 mm/s	41,23	2,7
100 mm/s	108,7	3,6
200 mm/s	101,2	2,8
300 mm/s	98,6	2,9
400 mm/s	97,7	2,5

Table 2: In this table the mean height profile and standard deviation for spanwise position 200 are shown.

Coater velocity	Mean of the height profile in μm	Standard deviation in μm
50 mm/s	130,2	2,5
100 mm/s	131,3	2,5
200 mm/s	124,4	2,1
300 mm/s	122,1	2,1
400 mm/s	121,4	2,1

Table 3: In this table the mean height profile and standard deviation for spanwise position 210 are shown.

6 Discussion and Conclusion

As already mentioned in chapter 2, there are two main tasks which are treated in this thesis. The first task is to determine the influence of the coater velocity on the height profile. When looking at the effect of velocity on the height profiles for 100 μm, almost no difference can be seen when altering the coater velocity. However, when looking at the influence of the coater velocity on the height profile in case of a coater height of 150 μm and 200 μm, one can see a small decrease in the height profile for a faster coater velocity. The decrease is not perfectly noticeable in the height profile figures 9a, 9b, 9c, 9d and 9e. The decrease can be seen better in the tables 4, 5 and 6. The formula derived in section 3.2 predicts a decrease in resin layer height for increasing velocity. Therefore, it can be concluded that the experimental values coincide well with this formula for layer height. The fact that the decrease of the height profile of the resin is not very well visible is probably due to the fact that all coater heights for which measurements are carried out, are relatively small. This means a change in velocity would have less effect on the height profile. Another observation to point out, is that in the case of a high coater velocity and a relatively small coater height, the thickness of the resin layer should go to half the coater height. When looking at the coater height of 200 μm, it is observed that the layer height will be approximately 100 μm. This is precisely as the formula for layer height derived in section 3.2 predicts. For the experimentally gathered data of the measurements for 150 μm, which can be found in Appendix B, it can be seen that the value of the layer height is approximately half the coater height, which is again as predicted. However for the measurements for a coater height of 100 μm, which can also be found in Appendix B, the value of half the coater height is nowhere to be found since the measured height profile is negative. Despite this illogical measurements, it can be concluded that formula (8) is in accordance with the experimentally determined values.

Another focus point of this thesis is to figure out if the 2D-assumption of the Comsol model discussed in section 3.5 is valid. To check this assumption, all measurements were compared to other measurements with the same circumstances but with a different spanwise position. The results of these measurements can be seen in figure 9 and tables 4, 5 and 6. When comparing these results, one can see that the height profiles do not look exactly alike. Furthermore, it can be seen that the height profiles in almost all measure-

ments of spanwise position 190 mm are lower than the height profiles of the measurements at the symmetry axis. Also, it can be noticed that all results of measurements at spanwise position 210 mm have a higher layer height. Therefore, it can not be concluded that this layer deposition process is truly symmetric based on these results. An explanation for these measurements could be that the Lepus Next Gen was not entirely spirit level. A slight error in this level might cause a discrepancy in these measurements. Another explanation could be the fact that the height profile measurements were not performed extremely fast, this may have caused settling effect of the resin to come into play.

The results gathered by the Comsol model are very logical. The model resulted in a resin layer of exactly half the coater height above the bottom plate. This result is predicted by formula (8). This is also the case for most of the gathered data. Therefore, the model is in good accordance with the experimental data gathered.

As one can see, most results found during this thesis are not perfect. First of all it can be clearly seen that the measurements for a coater height of 100μm, which can be found in Appendix B, are all negative. This is of course very unrealistic. Furthermore it can be noticed that every measurement fluctuates more than what was expected. Sometimes these fluctuations were up to 50 μm. At first sight 50 μm does not seem a lot, however if it is stated that the thickest layer is 200 μm it can be easily seen that 50 μm is a very large fluctuation in this case.

Furthermore, when carrying out the experiment, the plan at first was to measure resin with a viscosity of 1 Pa·s. However, at the time of the experiment the resin had not yet been delivered, so another type of resin was used. One of the drawbacks of using this resin was the significantly lower viscosity of which the exact value is not known. Furthermore, the resin which was used was not opaque. Even though this was not disastrous, it did decrease the accuracy of the confocal chromatic sensor a little. This could have caused the heavy fluctuations in several of the measurements.

Another point of discussion would be the filtering of the data. Some strange data has been found during the data filtering, this is visible as absurdly high and steep peaks. The most logical explanation for the peaks would be that the confocal chromatic sensor could not handle the rate of change of the

height profile. Therefore all the peaks were deleted and ignored for the rest of the measurements.

To have continuation of the experiments performed in this thesis, some further research can be done. One of the cases which needs to be further investigated is how the height profile will look for an even higher coater height above the bottom plate. This could be done at coater heights of approximately 1 mm. This research could give more insights into the correctness of formula (8), and would therefore be very interesting for the understanding of the problem. Another experiment which could be performed would be to investigate the effect of a cavity in the bottom plate on the deposited layer. In the following paper [4] the creation of deformations due to the coater passing over a cavity are discussed. The main focus of this research could be what effect the coater velocity has on the deformations that are created. This research could be really useful for making a system which is trying to prevent such mistakes.

References

[1] B.Dongen. Recoater measurements for the lepus next gen.

[2] M. A. Browne, O. Akinyemi, and A. Boyde. Confocal surface profiling utilizing chromatic aberration. *Scanning*, 14(3):145–153.

[3] H. J. Kim et al. Analytical fluid flow models for tape casting. *Journal of the American Ceramic Society*, 89(9).

[4] J.Senden. Design of a recoater concept for additive manufacturing of ceramics.

[5] Micro-Epsilon. Confocal sensor systems for displacement, distance, position and thickness.

[6] H. Narahara. Measurement of liquid surface unevenness in stereolithography. *JSME International Journal*, 47(1), 2004.

[7] A. Kozhevnikov R.P.J.Kunnen G. van Baars H.J.H. Clercx. Investigation of the fluid flow during the recoating process in additive manufacturing. *submitted to rapid prototyping*, 2019.

[8] Wikipedia contributors. Navier–stokes equations — Wikipedia, the free encyclopedia, 2019. [Online; accessed 17-June-2019].

[9] Wikipedia contributors. Phase field models — Wikipedia, the free encyclopedia, 2019. [Online; accessed 24-June-2019].

7 Appendices

A Preparing the measured data

In appendix A the processing of the data gathered will be discussed. When measuring the height profile, a lot of points will be measured to ensure a precise height profile. This means that there will be a lot of data points. To make the data usable some modifications have to be performed, however to do this by hand is too time consuming. Therefore, some MATLAB scripts have been written to fasten the data processing. In this chapter a look will be taken at all MATLAB scripts that have been used and it will be explained how these scripts work.

The first script was made to filter out some inexplainable peaks. When looking at the data some very steep and high peaks appeared, these peaks however are not physically explainable. The only explanation for this data to be true would be the existence of very small invisible holes in the bottom plate of the setup of about 2.1 m deep which would be rather unlikely. Therefore the first script which can be seen just below will search through the height profile and filter out all values above a certain threshold.

```
clear all;
for ii=1:16
iistr = num2str(ii);
load([iistr,'.mat'])
[rowIdcs, ¬] = find(Value{1,3}>4500000);
Value{1,1}(rowIdcs,:) = [];
Value{1,2}(rowIdcs,:) = [];
Value{1,3}(rowIdcs,:) = [];
Value{1,4}(rowIdcs,:) = [];
save([iistr,'filtered.mat']);
end
```

The second, third and fourth script are made with the same purpose, to split every measurement into three different measurements. The reason for splitting the measurements in three parts is that every measurement contains a measurement of the height profile along the moving axis of the coater three times. The three measurements were performed at different positions along the axis perpendicular to the coater's moving direction. To perform such a filtering, the scripts which can be seen below will search for the right axis and delete the rest of the data.

```
clear all;
for ii=1:16
iistr = num2str(ii);
load([iistr,'filtered.mat'])
```

```
[rowIdcs1, ¬] = find(Value{1,4}>190.1);
Value{1,1}(rowIdcs1,:) = [];
Value{1,2}(rowIdcs1,:) = [];
Value{1,3}(rowIdcs1,:) = [];
Value{1,4}(rowIdcs1,:) = [];
[rowIdcs2, ¬] = find(Value{1,4}<189.9);
Value{1,1}(rowIdcs2,:) = [];
Value{1,2}(rowIdcs2,:) = [];
Value{1,3}(rowIdcs2,:) = [];
Value{1,4}(rowIdcs2,:) = [];
save([iistr,'prepared190.mat']);
end
```

```
clear all;
for ii=1:16
iistr = num2str(ii);
load([iistr,'filtered.mat'])
[rowIdcs1, ¬] = find(Value{1,4}>200.1);
Value{1,1}(rowIdcs1,:) = [];
Value{1,2}(rowIdcs1,:) = [];
Value{1,3}(rowIdcs1,:) = [];
Value{1,4}(rowIdcs1,:) = [];
[rowIdcs2, ¬] = find(Value{1,4}<199.9);
Value{1,1}(rowIdcs2,:) = [];
Value{1,2}(rowIdcs2,:) = [];
Value{1,3}(rowIdcs2,:) = [];
Value{1,4}(rowIdcs2,:) = [];
save([iistr,'prepared200.mat']);
end
```

```
clear all;
for ii=1:16
iistr = num2str(ii);
load([iistr,'filtered.mat'])
[rowIdcs1, ¬] = find(Value{1,4}>210.1);
Value{1,1}(rowIdcs1,:) = [];
Value{1,2}(rowIdcs1,:) = [];
Value{1,3}(rowIdcs1,:) = [];
Value{1,4}(rowIdcs1,:) = [];
[rowIdcs2, ¬] = find(Value{1,4}<209.9);
Value{1,1}(rowIdcs2,:) = [];
Value{1,2}(rowIdcs2,:) = [];
Value{1,3}(rowIdcs2,:) = [];
```

```
Value{1,4}(rowIdcs2,:) = [];
save([iistr,'prepared210.mat']);
end
```

Lastly, a script was used to subtract the height profile of the resin from the dry height measurement. Although the concept is simple, it will be the most complex script. This is due to the fact that different measurements do not have the same number of data points, this is caused by different coater velocities during the measurement, and therefore a different velocity of the confocal chromatic sensor measuring the height profile. To solve the problem of incompatible data, the interpolate function provided by MATLAB will be used. This MATLAB script which can be seen below also automatically plots the absolute height profile created by the use of the interpolate function.

```
clear all
close all
ar = ["100","50","200","300","400","50",
"100","200","300","400","50","100","200","300","400"]
means = []
stds = []
for iiiiii=2:16
z = 0;
fig = figure();
hold all
for p=190:10:210
    z = z + 1;
    pstr = num2str(p);
    iiiiii2str = num2str(iiiiii);

        load(strcat('1prepareddataflat',pstr,'.mat'))
    x0 = double(Value{1,2});
    h0 = double(Value{1,3});

    F = strcat(iiiiii2str,'prepareddataflat',pstr,'.mat')
    load(F)
    x = double(Value{1,2});
    h = double(Value{1,3});

    if p < 191
       h0 = h0 + 20000;
    end

    if iiiiii > 6
        h= h-100000;
        disp(strcat('bij ', iiiiii,' eraf'))
```

```
32      end
33      if iiiiii > 11
34          h = h + 50000;
35          disp(strcat('bij ', iiiiii,' erbij'))
36      end
37      if iiiiii < 17
38          h = h *10^-5;
39          h0 = h0 *10^-5;
40      end
41      hinterp = interp1(x,h,x0);
42      dh = (h0 - hinterp)*10^-1;
43
44      heightname = ar(iiiiii-1);
45      graph1 = plot(x0,dh)
46      set(graph1,'LineWidth',4);
47
48
49      dhmin = dh(¬isnan(dh));
50      means(z,iiiiii-1) = mean(dhmin);
51      stds(z,iiiiii-1) = std(dhmin);
52
53
54
55  %     suptitle(strcat('height profile of the resin for a ...
        spanwise position of ',pstr))
56
57
58
59
60  end
61      legend('190 mm','200 mm','210 mm')
62      title(strcat('Height profile of the resin at a coater ...
            velocity of ',{' '},heightname,'mm/s'))
63      grid()
64      xlabel('Position along the moving axis in mm')
65      ylabel('Absolute height of the resin layer in mm')
66      %set(gcf, 'Position',  [100, 100, 1000, 400])
67      saveas(fig,strcat(iiiiii2str,'prepareddataflatint'
68      ,pstr,'.jpg'));
69      close all
70
71  end
```

B All results

In this appendix all results gathered during this thesis are shown. The first figure 10 shows the measurements with a coater height of 100 μm above the bottom plate. Furthermore, a measurement was performed at a coater height of 150 μm. The results can be seen in figures 11. Lastly, a measurement was performed at a coater height of 200 μm. The results can be seen in figure 12. Furthermore a table of the mean height and standard deviation of the 200 μm is also added.

Coater velocity	Mean of the height profile in μm	Standard deviation in μm
50 mm/s	82,4	8,2
100 mm/s	86,4	8,3
200 mm/s	74,1	7,5
300 mm/s	71,2	7,8
400 mm/s	70,5	6,9

Table 4: In this table the mean height profile and standard deviation for spanwise position 190 are shown.

Coater velocity	Mean of the height profile in μm	Standard deviation in μm
50 mm/s	41,23	2,7
100 mm/s	108,7	3,6
200 mm/s	101,2	2,8
300 mm/s	98,6	2,9
400 mm/s	97,7	2,5

Table 5: In this table the mean height profile and standard deviation for spanwise position 200 are shown.

Coater velocity	Mean of the height profile in μm	Standard deviation in μm
50 mm/s	130,2	2,5
100 mm/s	131,3	2,5
200 mm/s	124,4	2,1
300 mm/s	122,1	2,1
400 mm/s	121,4	2,1

Table 6: In this table the mean height profile and standard deviation for spanwise position 210 are shown.

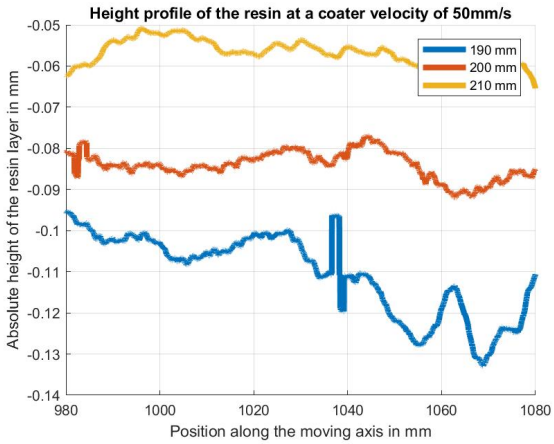

(a)

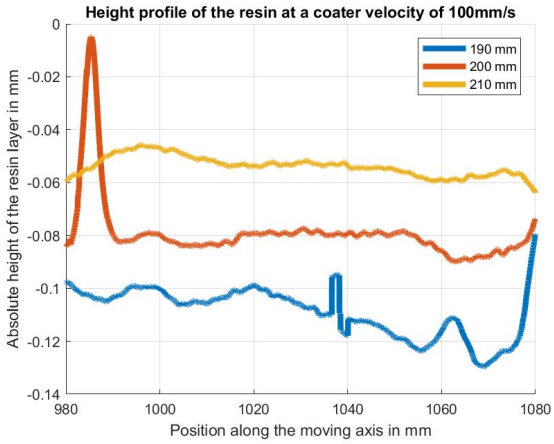

(b)

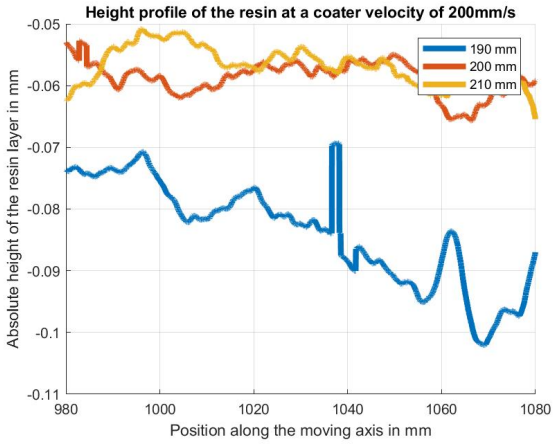

(c)

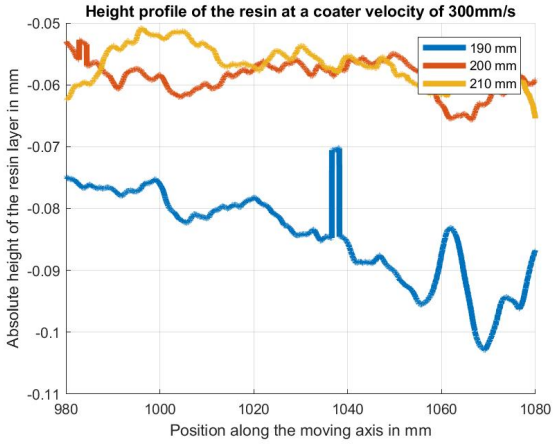

(d)

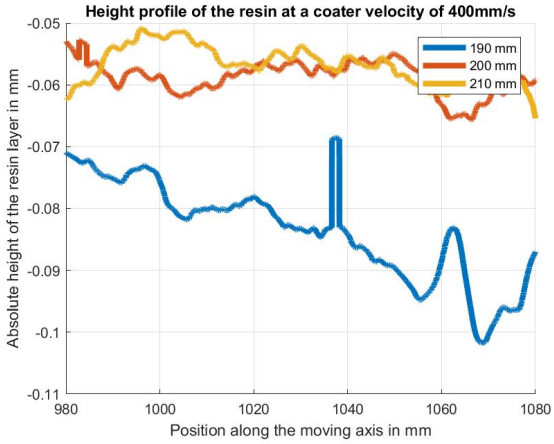

(e)

Figure 10: The absolute height profile of the resin with a coater height of 100 μm above the bottom plate and spanwise positions of 190 mm, 200 mm and 210mm and for five different velocities 50 mm/s, 100 mm/s, 200 mm/s, 300 mm/s and 400 mm/s. The spike in every 190 mm measurement is caused by a bump which was measured in the bottom plate.

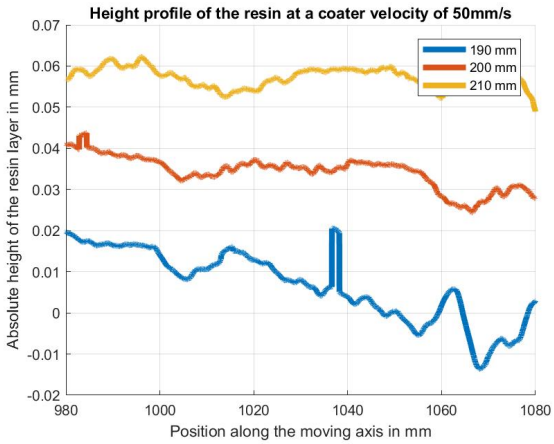

(a)

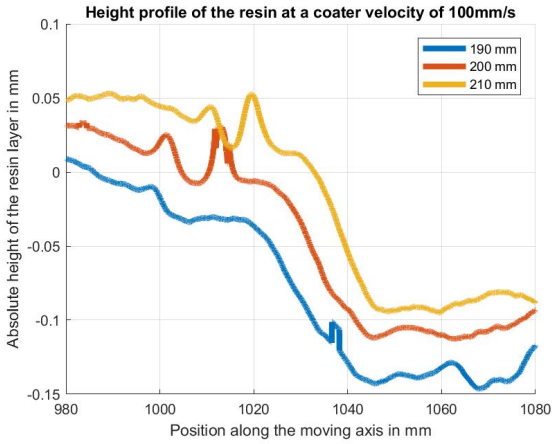

(b)

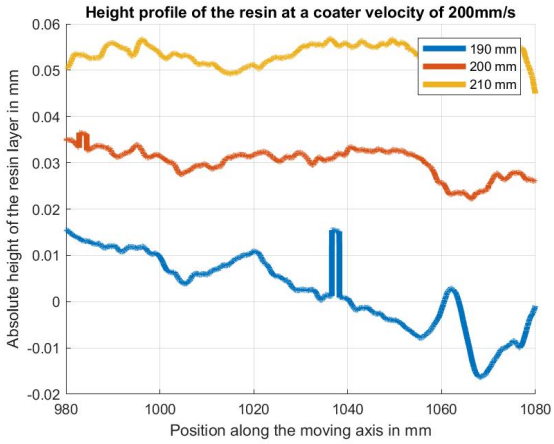

(c)

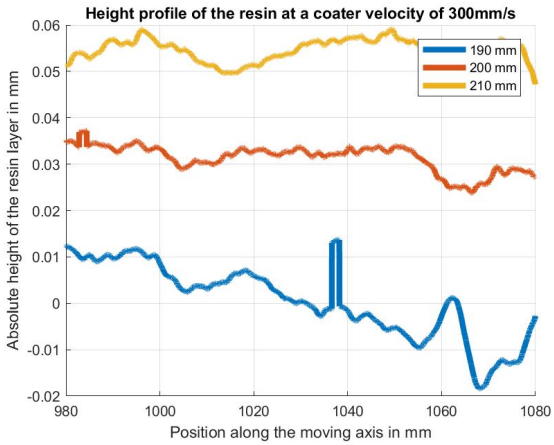

(d)

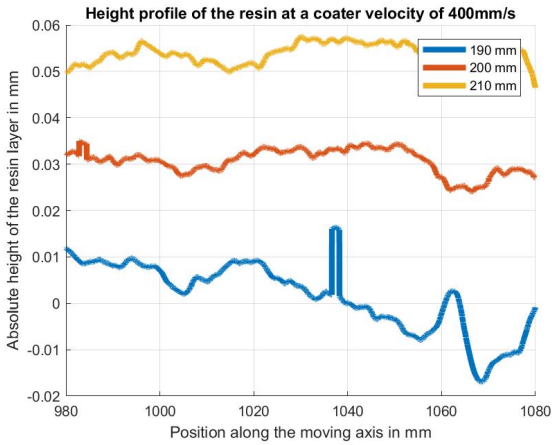

(e)

Figure 11: The absolute height profile of the resin with a coater height of 150 μm above the bottom plate and spanwise positions of 190 mm, 200 mm and 210mm and for five different velocities 50 mm/s, 100 mm/s, 200 mm/s, 300 mm/s and 400 mm/s. The spike in every 190 mm measurement is caused by a bump which was measured in the bottom plate.

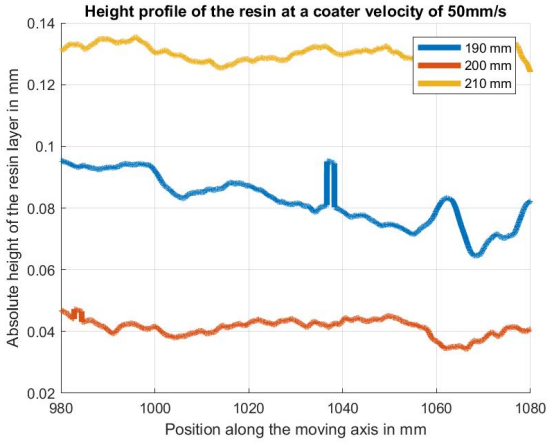

(a)

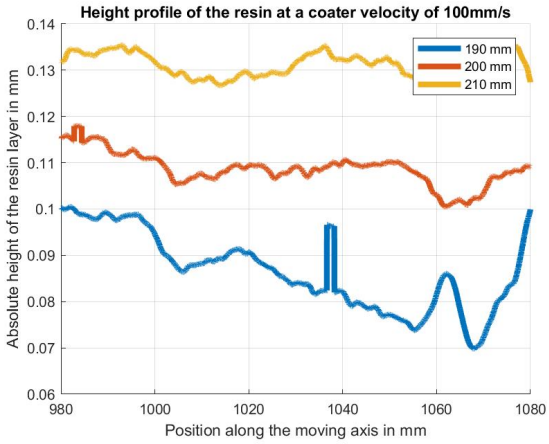

(b)

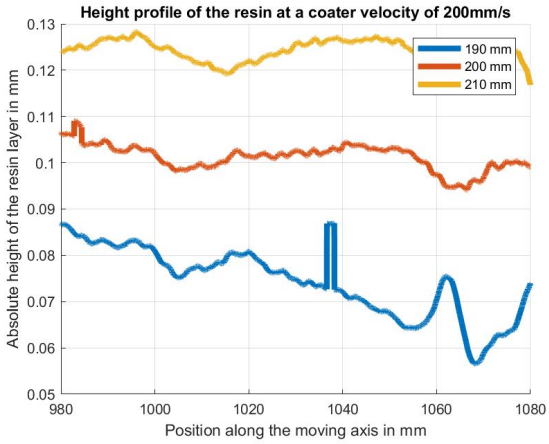

(c)

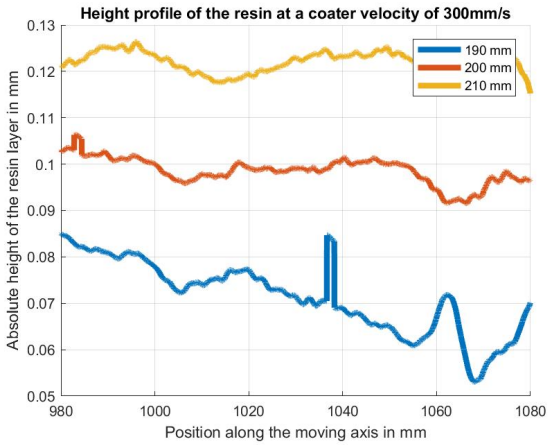

(d)

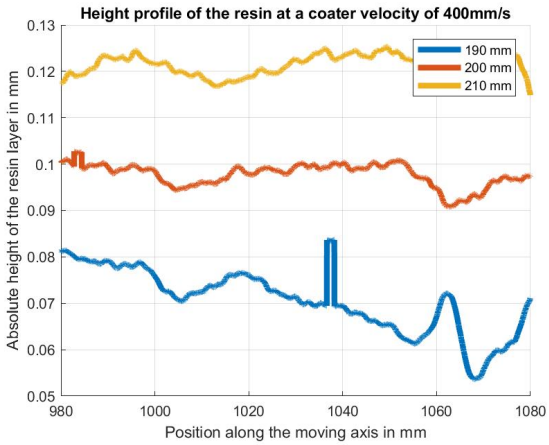

(e)

Figure 12: The absolute height profile of the resin with a coater height of 200 μm above the bottom plate and spanwise positions of 190 mm, 200 mm and 210mm and for five different velocities 50 mm/s, 100 mm/s, 200 mm/s, 300 mm/s and 400 mm/s. The spike in every 190 mm measurement is caused by a bump which was measured in the bottom plate.